

Received August 18, 2020, accepted August 28, 2020, date of publication September 2, 2020, date of current version September 17, 2020.

Digital Object Identifier 10.1109/ACCESS.2020.3021121

A Path Planning Method for V-Shaped Robotic Cutting of Nomex Honeycomb by Straight Blade Tool

RUOYU CUI¹, JIANFU ZHANG^{1,2}, (Member, IEEE), PINGFA FENG^{1,2,3},
DINGWEN YU¹, AND ZHIJUN WU¹

¹Beijing Key Laboratory of Precision/Ultra-Precision Manufacturing Equipments and Control, Department of Mechanical Engineering, Tsinghua University, Beijing 100084, China

²State Key Laboratory of Tribology, Department of Mechanical Engineering, Tsinghua University, Beijing 100084, China

³Division of Advanced Manufacturing, Tsinghua Shenzhen International Graduate School, Tsinghua University, Shenzhen 518055, China

Corresponding author: Jianfu Zhang (zhjf@tsinghua.edu.cn)

This work was supported in part by the National Natural Science Foundation of China under Grant 51761145103 and Grant 51875311, and in part by the Shenzhen Foundational Research Project (Subject Layout) under Grant JCYJ20160428181916222.

ABSTRACT V-shaped cutting by straight blade tool has been proposed as a typical process to quickly remove large volumes of Nomex honeycomb. To meet the process requirements of V-shaped cutting by robots, a major problem is that the six degrees of freedom of the straight blade tool must be precisely programmed. In this paper, a path planning method for the V-shaped robotic cutting process is presented. The determining method of path parameters for cylindrical parts is firstly analyzed, with an optimization model proposed. The position of path points is pre-generated by robotic machining module of CAM software, and machining files in the robot language are output. Considering the requirement of V-shaped cutting path, a special post-processing program is developed to translate the CAM software generated machining files into final files for V-shaped cutting, which converts the reciprocating milling path into the V-shaped processing path and adds the orientation data of the path points. Furthermore, the robot machining files generated by the post-processing program are verified in MATLAB. V-shaped cutting experiments on Nomex honeycomb were carried out using 6-axis robot and ultrasonic cutting system to verify the presented method. Results show that the cylindrical surface of the machined workpiece is consistent with the expectation.

INDEX TERMS Path planning, V-shaped cutting, Nomex honeycomb, robot processing, straight knife.

I. INTRODUCTION

Nomex honeycomb composite, which is made with Nomex aramid fiber paper coated with phenolic resin, is widely used in aircraft structural parts because of their light weight, high specific strength and great heat resistance. At the same time, it is a kind of soft and brittle material because the material has low stiffness in transverse directions [1]. The machining of this material is a challenge because of its composite paper and cell structure. The traditional processing method for this material is high-speed milling with special milling tools, which collapses honeycomb cells rather than cutting them, causing most material to rub on the tool for an extended period of time, and this kind of severe wear greatly reduces the tool life [2]. In addition, this process has low efficiency,

The associate editor coordinating the review of this manuscript and approving it for publication was Ming Luo.

and usually causes poor surface quality and dimensional accuracy, with serious dust pollution [3]. Ultrasonic cutting technology has been applied as an effective way to reduce cutting force and realize efficient processing of Nomex honeycomb material [4], which avoids severe friction interaction between the tool and the material, helping to improve tool wear and dust pollution, as shown in Fig. 1. Unlike most machining methods removing chips continuously, this process separates and removes the volume of material chunk by chunk, which presents a new challenge for path planning.

Ultrasonic machining tools for honeycomb materials mainly include straight blade tools and disc tools, where straight blade tools are often used for rough machining to quickly remove large volume of material, and can also be used for finish cutting of boundary contour [5], [6]. In rough machining, the shape of cutting chips and surface is V-shaped, hence it can be also called V-shaped cutting. Compared to



FIGURE 1. Comparison of chip formation between milling [7] and V-shaped cutting.

general machining methods with a tool rotation motion, the V-shaped cutting process with a straight blade tool requires to control the three orientation degrees of freedom (DOF) in a specific way as well as three translation DOFs to keep its blade direction consistent with the feed direction. The path planning for machining, which is a technology of automatic generating tool path according to the processed workpieces and technological requirements, plays an important role in achieving efficient manufacturing process. The current CAM technology supports the general processing methods removing material by rotation, including turning, milling and drilling. As a new technology of removing material chunk by chunk with straight blade tool, V-shaped cutting has different material removal form and tool motion compared with traditional methods, which is a novel issue for CAM technology research. As a rough machining process of honeycomb materials, this process requires a large number of tool paths, which is difficult to implement path planning by manual programming, and therefore it is an urgent problem to be solved for engineering application of the process.

As a newly proposed machining process, ultrasonic V-shaped cutting with straight blade tool has been widely concerned in terms of ultrasonic equipment system [8], [9], machining mechanism [5], [10] and experimental study [11], [12]. However, the above researches are based on one cutting feed, and the path planning method is not considered. Recently, there are some studies focusing on path planning for V-shaped cutting on machine tools. In some single-layer cutting and grooving cases, the process path is relatively simple and easy to plan manually. Zhang *et al.* [13] developed a CATIA-based resource library for motion control of ultrasonic machine tools. Cutting procedure and path of some typical parts were proposed [14], [15]. However, in multi-layer and large-volume cutting situation, path planning needs to be generated automatically. Yu *et al.* [16] studied theoretical method and machining efficiency of path planning. Chen [17] and Liu *et al.* [18] studied the planning method and generated tool path by secondary development in NX. The current reported studies of path planning for V-shaped

cutting process mostly focus on the principle analysis. The path generating method and the influence of path parameters on machining efficiency are not considered comprehensively.

There are two common cutting processes with straight blade tool. One is used for the contour cutting of thin work-piece which only needs single-layer cutting move, as shown in Fig. 2 (a). When performing V-shaped cutting, the straight blade tool is used for single-layer cutting first, and then the disc tool is used for surface cleaning, as shown in Fig. 2 (b). The process requires two kinds of tools to switch between each cutting layer, causing low machining efficiency, and there is a lack of automatic path programming methods as well.

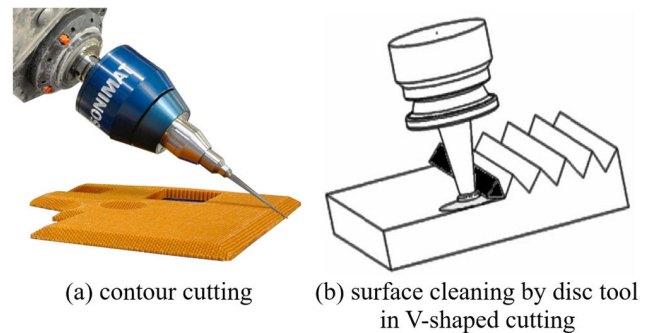


FIGURE 2. The cutting process with straight blade tool [19], [20].

In addition to the immaturity of path planning technology, the special ultrasonic cutting machine tool that supports 6-DOF control has a very high cost, which further limits the application of V-cutting. Compared with machine tool, 6-DOF industrial robot can directly control the direction of the tool blade flexibly at low cost. The application of industrial robots is proven, and robot system equipped with ultrasonic cutting effector for V-shaped cutting has a low cost and can achieve more working space through external axis when processing large structures. The disadvantage of using robots for machining is their low stiffness and accuracy [21], whereas the cutting force of the ultrasonic cutting process for Nomex honeycomb is small enough [22] to meet the accuracy of robot. At present, the studies of robotic machining path planning focus more on robotic kinematic optimization on machining efficiency [23] and accuracy [24], [25], and the tool path is usually generated by general CAM system [24], [26], [27]. However, V-shaped cutting requires special path planning method as mentioned above, and there are few or no reports on the V-shaped path planning for robots at present. The path planning of V-shaped robotic cutting has not been reached, which is one of the critical problems for application of this process.

In conclusion, the previous research on V-shaped cutting path planning of machine tools and robots is insufficient in path parameter determination, automatic path generation and post-processing method, which is difficult to meet the actual application. In addition, relying on disc tools for surface cleaning in V-shaped cutting severely restricts

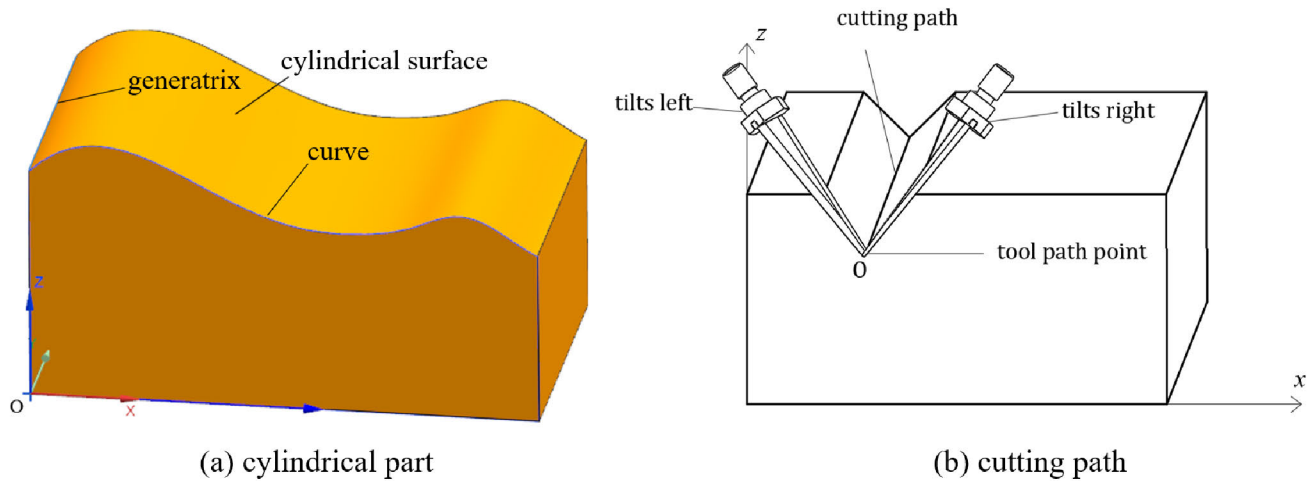


FIGURE 3. V-shaped cutting surface.

the efficiency. To solve the above problems, a path planning and generating method for V-shaped robotic cutting of Nomex honeycomb by straight blade tool is proposed in this paper, which allows the straight blade tool to completely replace the milling tool for roughing and avoids the use of disc tools for surface cleaning between each cutting layer, improving the machining efficiency. Firstly, it analyzes configuration type and the key geometry parameters of the V-shaped cutting path. The machining files are pre-generated as a form of three-axis milling process in NX, a general CAM software in Section 2, and then post-processed into V-shaped cutting process by a post-processing program developed in Section 3. To verify the path planning method, robot machining experiments are carried out and experimental results are discussed in Section 4.

II. TOOL PATH PLANNING METHOD

A. V-SHAPED CUTTING PATH CONFIGURATION

In the aerospace industry, Nomex honeycomb materials are generally used in fuselage structures such as skins and spoilers, which are geometrically characterized by cylinders with small curvature (cuboids included). A typical cylindrical part has a curved surface formed by a generatrix moving parallel along a curve, as presented in Fig. 3 (a). V-shaped cutting by straight blade removes the material for rough machining, as shown in Fig. 3 (b). One cutting path (parallel to y-axis in the figure) is repeated twice: the cutting tool tilts left at first, and feeds along the path; then tilts right with tool tip position kept fixed, and feeds back again along the same path to cut off a piece of material. The V-shaped cutting process is completed by repeating the above-mentioned cutting motion.

For cylindrical parts, the cutting paths are linear and parallel to coordinate axes. The horizontal cutting layers, where the cutting paths are planned with a fixed step, are established with fixed layer spacing. Neglecting the thickness of the blade, straight blade tool is projected as a straight line on x-z plane, and the cutting paths are projected as a lattice

composed of discrete tool points on x-z plane. Three types of lattices are proposed: orthogonal lattice, interlaced lattice, and free lattice, as shown in Fig. 4 (a), (b), (c). Red diagonal lines represent the cutting tool positions, the circles are cutting path points.

Lattice configuration affects the efficiency and scallop height of the process. From the perspective of processing scallop height, in orthogonal lattice and interlaced lattice, the x coordinates of path points on each cutting layer are fixed, and can't be adjusted according to contour of the workpiece, causing high scallop height. Whereas in free lattice the x coordinates on each layer are free and not related to others, and can be adjusted according to the contour of the workpiece, thereby reducing the scallop height. From the perspective of processing efficiency, layer spacing is constrained by the available cutting length of the tool. The cutting length (length of red diagonal lines in Fig. 4) of the interlaced lattice is equal for each cutting, and for this reason, the length of the tool can be fully utilized, and layer spacing can be maximized with given tool length, which means interlaced lattice has the highest efficiency. The same analysis shows that orthogonal lattice takes second place, and free lattice's efficiency is lowest, with layer spacing 50% lower than that of interlaced lattice.

B. DETERMINATION OF TOOL PATH PARAMETERS

The geometry parameters of the V-shaped cutting process are shown in Fig. 5. The length L of OB is the actual cutting length of the blade. For ultrasonic vibration, the amplitude gets the largest at the tool tip and gradually decreases along the blade, and the cutting length L is required to ensure enough amplitude, that is $L \leq L_{\max}$. The length d of OA is the projection of the cutting length in x-z plane; θ is the tool's rake angle; α is the swing angle; h is the layer spacing; s is the step size of tool path; β is the half apex angle of the straight blade tool; and b is the extension length. The

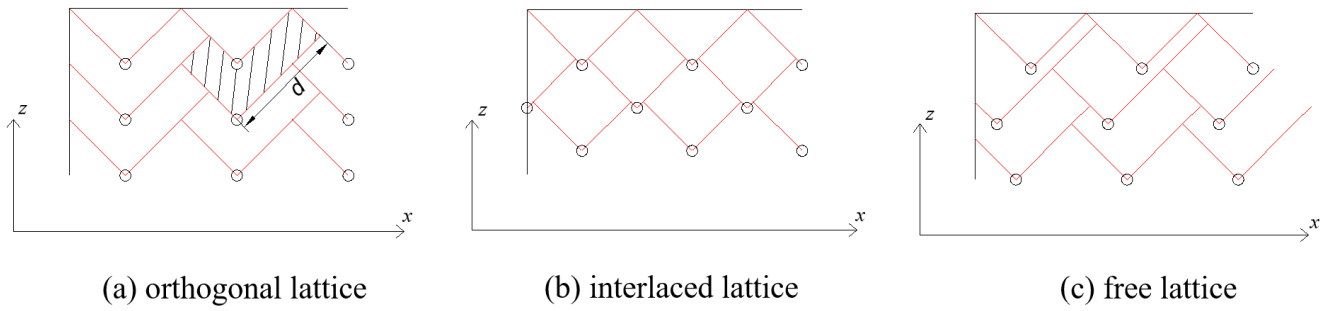


FIGURE 4. Lattice configurations of V-shaped cutting path.

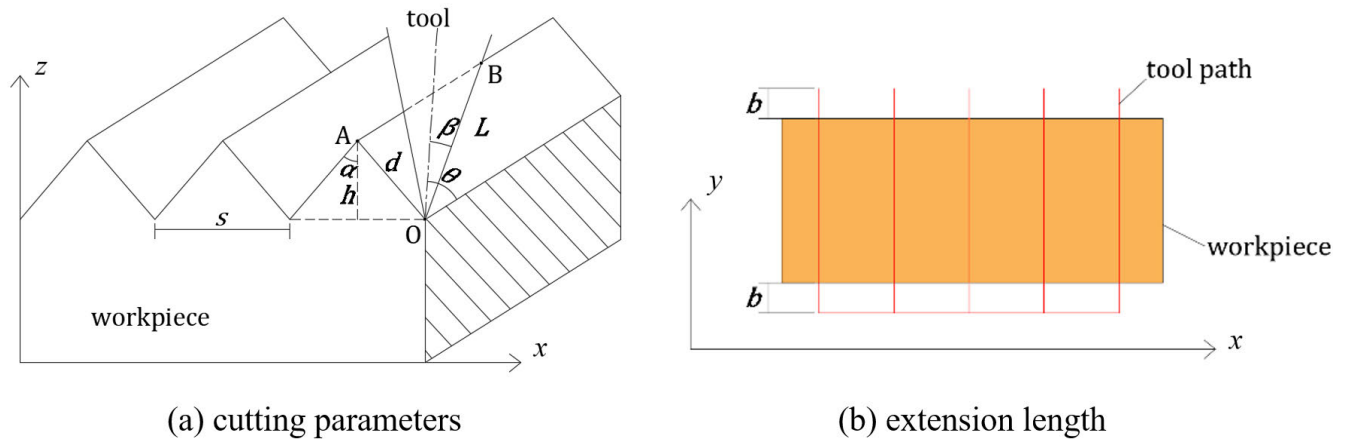


FIGURE 5. Geometry parameters of the V-shaped cutting process.

parameters required for tool path planning include rake angle, swing angle, layer spacing, step size, and extension length.

Rake angle θ , between the tool axis and the cutting direction, affects the components of the cutting force, which influences the acoustic performance of the ultrasonic vibration system and the stability of the cutting process.

Swing angle α is the angle between the tool plane and the normal vector of the cutting surface (z-axis in Fig. 5 (a)). Since angles of the V-shaped cutting grooves are equal to 2α , swing angle determines the shape of cutting chips, and effects machining efficiency consequently. Taking the orthogonal lattice as an example, a chip unit, which is shown as the shaded part of Fig. 4 (a), has a cross-section area Q given as:

$$Q = \frac{4}{9}d^2 \cdot \sin 2\alpha \quad (1)$$

where d is projection of cutting length:

$$d = L \cdot \sin(\theta - \beta) \quad (2)$$

therefore:

$$Q = \frac{4}{9}L^2 \cdot \sin^2(\theta - \beta) \cdot \sin 2\alpha \quad (3)$$

where L is the cutting length of the tool. The equation (3) shows that, if given cutting length, the cross-section area of

the chip is related to the swing angle α , and gets maximum when $\alpha = 45^\circ$, which means high cutting efficiency.

The swing angle also needs to be considered according to the maximum inclination of the cutting surface. When machining steep surface, swing angle exceeding the maximum inclination of the surface may lead to unreachable areas, that means $0 < \alpha \leq \alpha_{\max}$.

Layer spacing of orthogonal lattice depends on cutting length, swing angle, half apex angle and rake angle:

$$h = \frac{2}{3}L \cdot \cos \alpha \cdot \sin(\theta - \beta) \quad (4)$$

Extension length b is the safe distance between workpiece and tool tip position of non-cutting path to avoid collision when tool reaches endpoints of cutting path, moves without cutting and adjusts its tilt orientation, as shown in Fig. 5 (b). The condition that no collision occurs is that b is greater than the y-axis projection component of cutting length L :

$$b = L \cdot \cos(\theta - \beta) \quad (5)$$

Step size s depends on the swing angle and the layer spacing if tool paths don't overlap:

$$s = 2h \cdot \tan \alpha \quad (6)$$

Overlapping tool paths can be used to reduce the scallop height. Step size of tool paths with an overlap ratio ε is:

$$s = 2(1 - \varepsilon)h \cdot \tan\alpha \quad (7)$$

where $0 \leq \varepsilon < 1$. Higher overlap ratio leads to smaller step size and longer machining path.

Based on the above analysis, the tool path parameters are determined as the steps in Fig. 6.

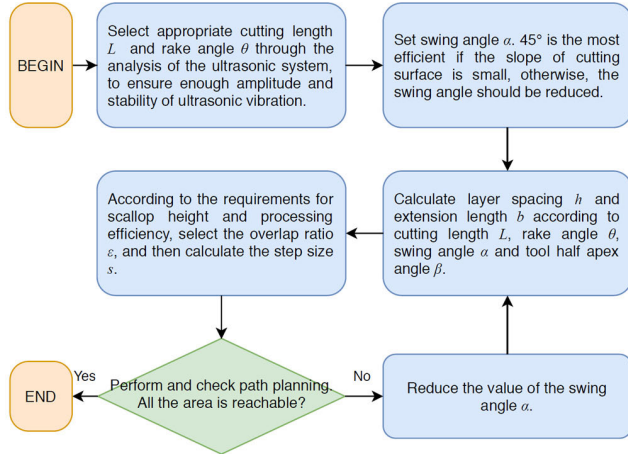


FIGURE 6. Diagram of determining tool path parameters.

C. PARAMETER OPTIMIZATION OF TOOL PATH

The last section analyzed the basic determination method of path parameters, that L_{max} , β , θ are given as known variables by the design of ultrasonic cutting system, and α , h , s are three independent path parameters with constrained value ranges. In order to find the best parameters with the highest machining efficiency, an optimization model of tool path parameters is established to minimize the processing time. V-shaped cutting is in the form of discrete lattice, so there are discontinuous mathematical relations between path parameters and evaluating indicators. In this paper, the mean value estimation is used to establish the mathematical expression of the processing time with the path parameters.

When a cutting path point interferes with the workblank boundary, the point is actual, but when a path point interferes with the contour surface of the part, the point is false. Through probability analysis of the point distribution, for given cutting height H_C and workblank width W , the average number of point layers is $\hat{n} = \frac{H_C}{h} - 0.5$, and the average number of point rows is $\hat{m} = \frac{W}{s} + 0.5$. Generally, the cutting height is estimated to be $\hat{H}_C = \frac{A_C}{W}$, where A_C is the projected area in x-z plane to be machined. therefore, the number of cutting path points \hat{N} is estimated as:

$$\begin{aligned} \hat{N} &= \hat{m}\hat{n} \\ \hat{n} &= \left(\frac{W}{s} + 0.5\right) \\ \hat{m} &= \left(\frac{A_C}{Wh} - 0.5\right) \end{aligned} \quad (8)$$

In the processing, all paths are linear movements. The processing time includes the cutting time of cutting path points and the moving time between different layers. The cutting time for each cutting path point consists of three parts: two feedings at the point, a posture adjustment between the two feedings, and a simultaneous adjustment of posture and position when moving to the next point:

$$t_1 = \frac{2D + 4b}{v_1} + \frac{2\arccos(\cos\alpha \cdot \sin\theta)}{\omega} + \max\left\{\frac{2\arccos(\cos\alpha \cdot \sin\theta)}{\omega}, \frac{s}{v_2}\right\} \quad (9)$$

where D is the workblank size in y direction, extension length $b = L \cdot \cos(\theta - \beta) = \frac{3 \cot(\theta - \beta)}{2 \cos\alpha} h$, v_1 is the average cutting speed of tool, v_2 is the average non-cutting moving speed, and ω is the average angular speed.

The moving time between different layers consists of two vertical movements and one horizontal movement, estimated as:

$$\hat{t}_2 = \frac{2h_0 + 2A_C/W + W - h - 0.5s}{v_2} \quad (10)$$

where h_0 is the distance from the safety plane of horizontal movement to the workblank.

The total processing time is got from equation (8-10):

$$\hat{T} = \hat{N}t_1 + \hat{m}\hat{t}_2 \quad (11)$$

It should be noted that the additional vertical movements caused by the contour undulation of the part surface are ignored in the above analysis, so the value is underestimated.

Since the V-shaped cutting process is used as rough machining, and the surface machined by V-shaped cutting process will be finished by disc tool, the scallop height of V-shaped cutting is a constraint index to be considered which has an effect on the finishing process. The scallop height δ is defined as the height of scallop area in the normal direction of the theoretical contour curve. Through the analysis of cases of scallop area, it can be concluded that the maximum scallop height in the extreme case is equal to the distance from a tip of V-shaped cutting contour of a cutting layer to the nearest theoretical cutting path point of the next layer, as:

$$\begin{aligned} \delta &= \sqrt{\frac{1}{4}s^2 + (2 - \varepsilon)^2 h^2} \\ &= \sqrt{\frac{1}{4}s^2 + \left(\frac{s}{2h \cdot \tan\alpha} + 1\right)^2 h^2} \end{aligned} \quad (12)$$

As a constraint index, the scallop height is limited by the process requirements of disc tool, thus:

$$\delta < \delta_{max} \quad (13)$$

TABLE 1. The parameters and solutions of optimization.

	Size of workblank	Safety distance	Rake angle	Half apex angle
Given conditions	85×50×50mm	10mm	60°	7.13°
	Machined area	Cutting speed	Non-cutting speed	Angular speed
	3137mm ²	200mm/s	200mm/s	90°/s
Constraint conditions	Maximum scallop height	Maximum cutting length	Maximum Swing angle	
	10mm	10mm	50°	
Path parameters		Layer spacing	Step size	Swing angle
	Initial value	3mm	6mm	45°
	Optimization solution	4.40mm	5.97mm	34.16°

Therefore, the optimization model of tool path parameters has a form of nonlinear constrained optimization problem:

$$\begin{cases} \min \hat{T}(h, s, \alpha) \\ \text{s.t. } 0 < \alpha \leq \alpha_{\max} \\ 0 < h \leq \frac{2}{3}L_{\max} \cdot \cos \alpha \cdot \sin(\theta - \beta) \\ 0 < s \leq 2h \cdot \tan \alpha \\ \delta \leq \delta_{\max} \end{cases} \quad (14)$$

The h , s and α are the independent variables, and the expressions of the intermediate variables are given by equation (8-12). The analysis shows that the scallop height, which is the main factor affecting finish machining process, mainly depends on overlap ratio, step size and layer spacing. Taking small step size and layer spacing can reduce the scallop area, but it will lead to a reduction of the processing efficiency. By solving the optimization model of path parameters, the optimal processing efficiency can be given under the condition of the process constraints.

There are many algorithms for solving nonlinear constrained optimization problem. The optimization is carried out based on interior point algorithm in this paper. A set of initial solutions of path parameters is given as the start point of the iterations. The condition parameters and optimization solutions are given in Table 1. The initial path parameters are $h = 3\text{mm}$, $s = 6\text{mm}$ and $\alpha = 45^\circ$, and the optimized parameters solved by the iteration algorithm are $h = 4.40\text{mm}$, $s = 5.97\text{mm}$ and $\alpha = 34.16^\circ$. The theoretical processing times and the scallop areas of two sets of the parameters are compared in Fig. 7. Compared with the initial parameters, the optimized parameters reduce the processing time by 40.3%; the scallop height is increased, still within the constraint of $\delta_{\max} = 10\text{mm}$. The optimized parameters increase the layer spacing and step size to reach the constraint boundary of cutting length, decreasing the path

number consequently. The posture adjustment time is reduced by decreasing the path number and the swing angle which affects the range of posture adjustment. The cutting time and layer transfer time is reduced by decreasing the path number.

D. PRE-GENERATION OF TOOL PATH

Compared to general machining methods, the straight blade tool in the V-shaped cutting process has a special form of motion, including adjusting the swing angle and the rake angle, keeping the tool plane parallel with moving direction, feeding twice along one cutting path and some other details, which means a special path planning method must be used. In order to solve this problem, we propose a method that general CAM software is used to carry on path planning preliminarily, followed by special post-processing. As a general-purpose CAM software, NX was used for path planning in this work. Firstly, the cutting path is planned according to a three-axis reciprocating milling process corresponding to the determined tool path parameters, and then robotic machining file is output.

At first, the part and workblank model to be processed are imported into NX, and then a conical milling tool is configured corresponding to tool parameters including cutting length L and swing angle α . The conical shape of the tool is used to simulate the V-shaped cutting effect, so the cone angle should be twice the swing angle, and the tool length should be longer than cutting length. A KUKA robot model is imported as the machine tool of the process. Because NX is used only for the motion information of the tool path, and the coordinate data of the tool position are based on the workpiece coordinate system, which will be calibrated in machining, the specific position of the robot does not need to be accurate.

After that, the tool path can be generated in a three-axis reciprocating milling process according to the tool path parameters. Set straight line as the path form, and therefore the final exported file only consists endpoints of each straight path. The tool path is generated as Fig. 8 (a). After configuring the motion rules of the robot correctly, the cutting process is simulated as Fig. 8 (b), where blue areas means scallop area. Finally, the robotic machining file in KUKA robot language is generated and output.

III. POST-PROCESSING FOR V-SHAPED CUTTING

A. POST-PROCESSING METHOD AND PROGRAMMING

A post-processing method is proposed to convert the robotic file of three-axis reciprocating milling process to file of V-shaped cutting process. A post-process software is developed, in which codes of robot files are recognized and modified according to the V-shaped cutting parameters. In addition, necessary interactive graphical interface functions are developed as well. The main functions of post-process software include the following parts:

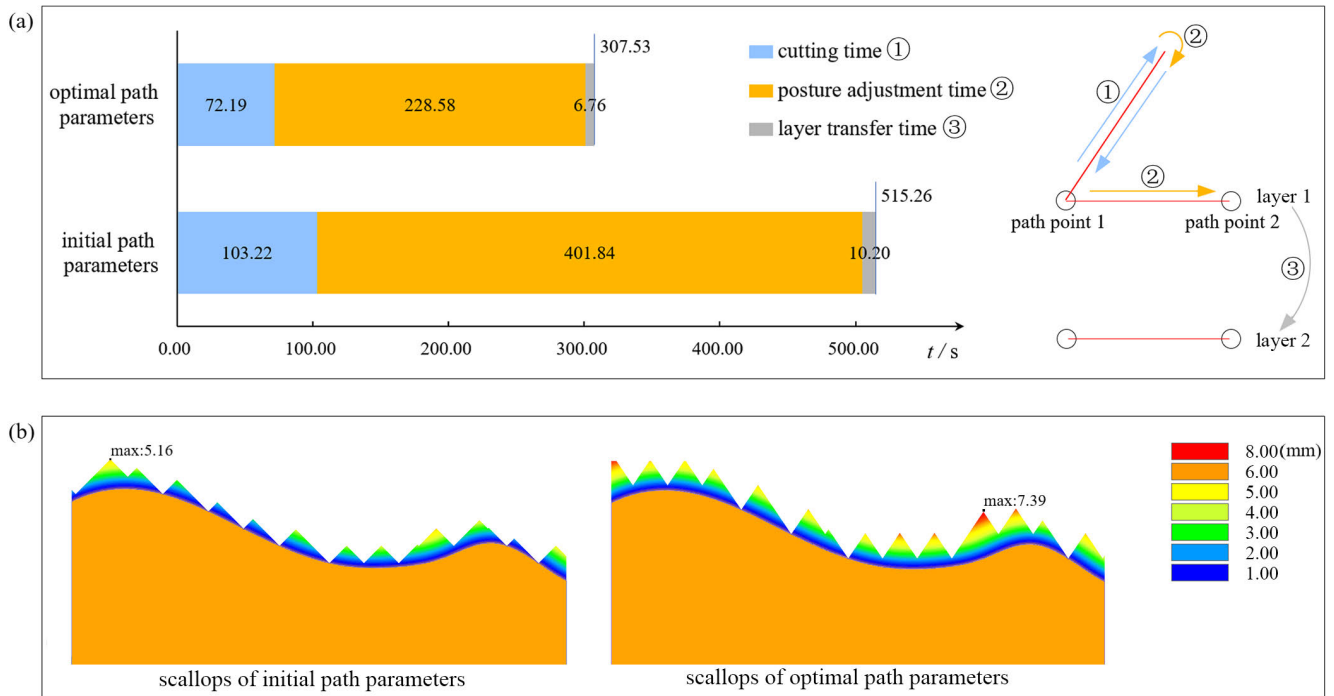


FIGURE 7. The processing times (a) and scallops (b) of initial parameters and optimized parameters.

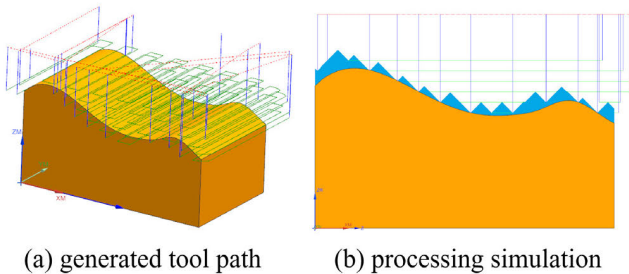


FIGURE 8. The path pre-generating in NX.

- 1) Read the robot machining files generated previously by NX software, and write codes into new files after the conversion process.
- 2) Relevant parameters are input in GUI, including file name to be post-processed, the path parameters (rake angle, swing angle, and extension length) and necessary geometric parameters (such as initial y coordinate, workpart height and width).
- 3) Process the tool path according to the V-shaped cutting requirements. Convert the reciprocating milling motion to the V-shaped cutting motion, as shown in Fig. 9.
- 4) Add the orientation data of paths according to path parameters.

The GUI of the post-processing program is developed based on Qt code base. The relevant parameters required for post-processing are input by the user in the interface.

In post-processing, the program reads the robot machining file line by line as statements, recognizes and converts each line of file text, and then writes into a new robot file as

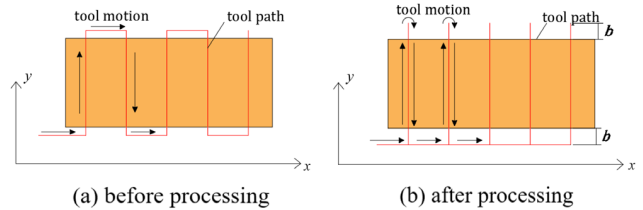


FIGURE 9. Processing of the tool path.

V-shaped cutting process. For each line of text, the post-processing steps are shown in Fig. 10. The detailed steps are as follows:

- 1) Judge whether the statement is a tool path point. Screen the statements of tool path point by noticing that path point statements start with “LIN” or “PTP”, modify the statements of tool path points and ignore other irrelevant statements.
- 2) Extract x, y and z coordinate values. Locate and extract three coordinate data by string recognition ways, and then convert them to number formats.
- 3) Reassign y coordinate values according to the extension length b , so that the path points are located at a distance b on both sides of the workpiece.
- 4) Calculate Δy , the difference of y values between the current point and the previous point, and then adjust all the y values to one side of the workpiece.
- 5) Judge whether the current point and the previous point constitute a cutting path. The Δy of cutting path is

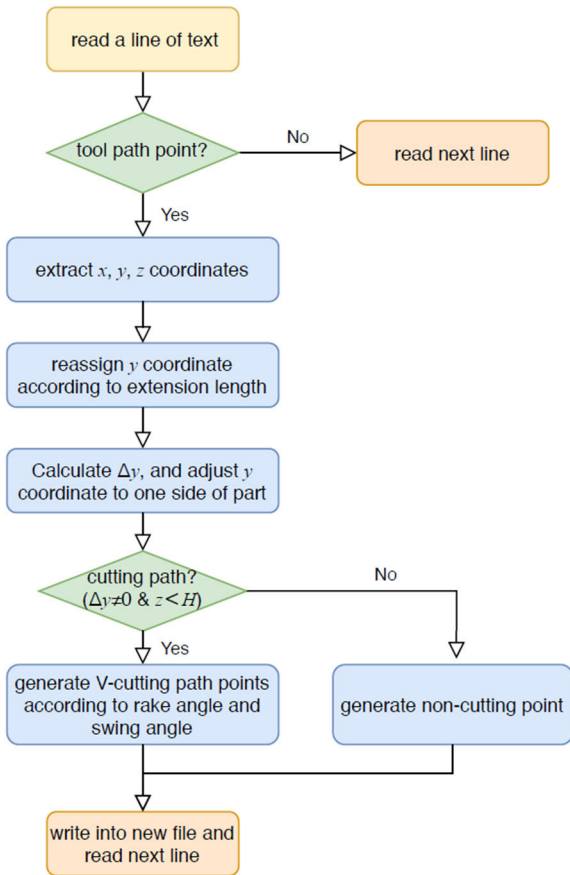


FIGURE 10. Diagram of post-processing path statements.

not zero, and the z coordinate value of cutting path is smaller than height of workblank. The reason to consider z coordinate value is, when the tool moves between different cutting layers, the Δy is also not zero, but it is not cutting path, and in this case, the z value is bigger than the height of workblank.

- 6) For a cutting path, according to the rake angle and swing angle, four path point statements are generated successively: left tilt, cutting move, right tilt and cutting move back. For a non-cutting path, the original point statement is generated. The generated statements are written into a new robot machining file.

In addition to post-processing the path statements, the program also generates initialization, speed definition and other necessary statements for the robotic files. The coordinate parameters of tool coordinate system and base coordinate system will be determined by calibrations in experiments.

B. KINEMATIC SIMULATION VERIFICATION

To verify the correctness of the robot machining files generated by the post-processing program, the position and orientation coordinates of all tool path points are exported from the post-processing program, and simulated based on a

kinematic robot model established in MATLAB. A 6-axis kinematic model of KUKA KR2210 robot, which is used in the experiment, is built by DH parameters (Denavit–Hartenberg parameters) in Robotic Toolbox based on Corke’s work [28]. The DH parameters, which include parameters of each link, and variable limits of each joint, are used to describe kinematic geometry of robots.

The simulation is realized by kinematic transformation and calculation. The coordinates of the path points imported into the simulation are transformed from the E6POS (Euler angles, 1×6) format of robot language to the SE3 (homogeneous transformation matrix, 4×4) format for subsequent calculations. Since the coordinate values of the path points are the tool coordinates in workpiece coordinate system, coordinate system transformation is performed first to obtain the tool coordinates in world coordinate system. In this coordinate mode, each straight path is interpolated to obtain a series of dense points of the tool between two original path points. Then, the coordinate values are transformed into the flange coordinates in world coordinate system, and in this coordinate mode the joint variables are calculated through inverse kinematic solution, driving the robot model to move, as shown in Fig. 11. The motion simulation shows that robot’s motion accords with the expectation of V-shaped cutting process.

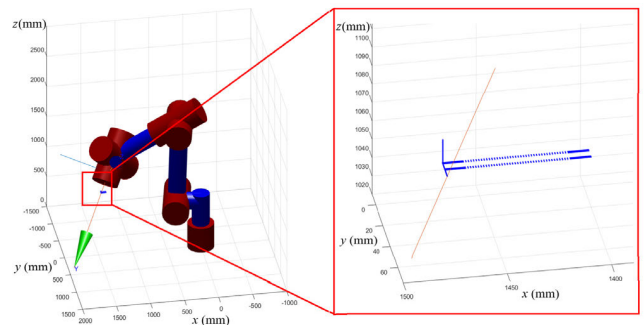


FIGURE 11. The motion simulation of cutting process.

The machined contour is simulated by 2D graphic calculation based on the tool path coordinate data and the workblank model in MATLAB. The simulation results of the machined contour and tool paths are shown in Fig. 12. Blue lines mean the tool paths generated by post-processing, and as a comparison, the red lines mean the tool paths generated by NX. The difference between the two paths indicates the effect of post-processing for V-shaped cutting. Simulation results of machined contour verify the accuracy of the robot machining files generated by the post-processing program.

IV. EXPERIMENTAL VERIFICATION

A. ROBOT MACHINING EXPERIMENTS

An experiment on KUKA KR2210 robot is conducted to verify the path planning. KR2210 is a 6-axis industrial robot with a maximum load of 210kg and a maximum arm length

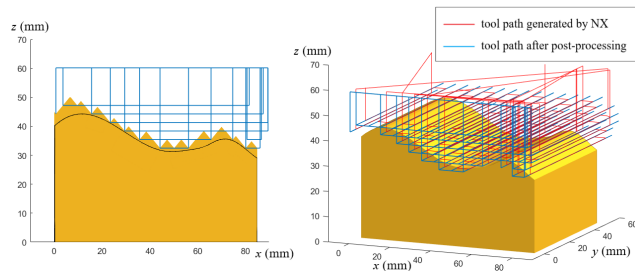


FIGURE 12. Tool path and machined contour simulated in MATLAB.

of about 3m. Based on Ma's work [29], ultrasonic system consisting of a shell, a transducer, a horn, and a straight blade tool, is assembled on the robot flange, as shown in Fig. 13.



FIGURE 13. Experiment system.

The ultrasonic generator provides an AC voltage signal, and the output amplitude of the transducer is amplified and transmitted to the tool by the horn. The material of work piece is ECA 1/8-3.0 hexagon honeycomb core, whose mechanical properties are shown in Table 2. The workpiece with the size of $85 \times 50 \times 50$ mm is fixed by means of fixture clamping, and the bottom of honeycomb cells is filled with sand to increase its stiffness. Before machining, the tool coordinate system and workpiece coordinate system are calibrated.

The machining file is imported into the robot controller system, and the machining process is carried out after calibration configurations. The machining motion of the robot is consistent with simulation in MATLAB. The cutting

TABLE 2. Material properties of Nomex honeycomb.

Property	Unit	Value
Cell diameter	mm	3.2
Density	kg/m ³	48
Compression strength in fiber direction	MPa	2.10
Shear strength in L-direction	MPa	1.32
Shear strength in W-direction	MPa	0.72
Shear modulus in L-direction	MPa	48
Shear modulus in W-direction	MPa	30

experiments were carried out and the machined surface of the work piece was achieved, as shown in Fig. 14 (b).

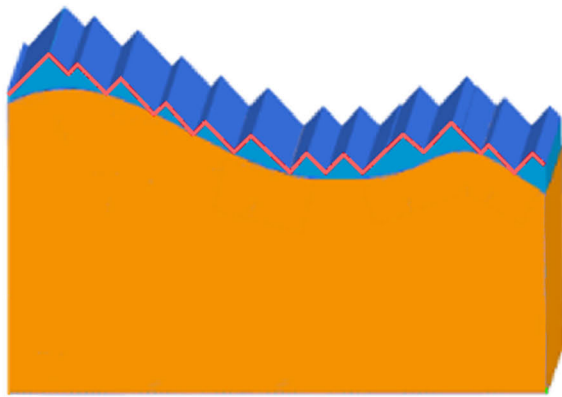
B. DISCUSSING

In order to quantitatively verify the experimental results, the contour curve of the machined surface was extracted, and the similarity between the experimental curve and the theoretical curve was evaluated by cross-correlation coefficient. The key contour points in the image are extracted, and then 1000-point theoretical contour curve and experimental contour curve are created by linear interpolation, as shown in Fig. 14. To evaluate the similarity of the two curves, the normalized cross-correlation function of two sets of data is obtained:

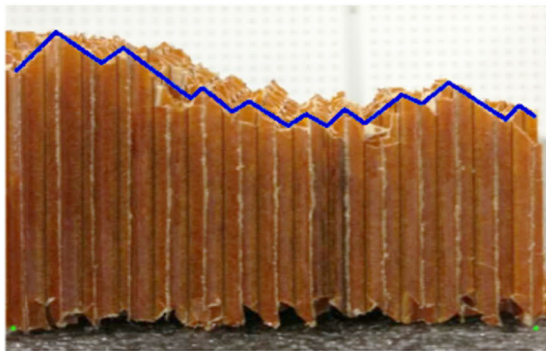
$$R'_{xy}(n) = \frac{1}{\sqrt{R_{xx}(0)R_{yy}(0)}} R_{xy}(n) \quad (15)$$

where n is point series, R_{xx} and R_{yy} are autocorrelations, and R_{xy} is cross-correlation. The value range of normalized cross-correlation is -1 to 1 , where 1 means the two sets of data are identical, 0 means no correlation, and -1 means the opposite. The function result is shown in Fig. 15, and the correlation coefficient between two curves, which is the maximum value of normalized cross-correlation, is 99.98%, which means that the machined contour and theoretical contour are extremely consistent. Furthermore, the profile tolerance of the two curves is analyzed. Calculation shows that the two curves have the maximum deviation (maximum distance from points on one curve to another curve) of 1.94mm, and correspondingly the profile tolerance of V-shaped cutting process given by manufacturer is 4mm, which means it basically meets the accuracy requirement. The main error sources are surface defect, which is caused by insufficiency of ultrasonic vibration, and the error of contour extraction. By improving the amplitude of the equipment system to improve the surface quality, the profile error can be reduced.

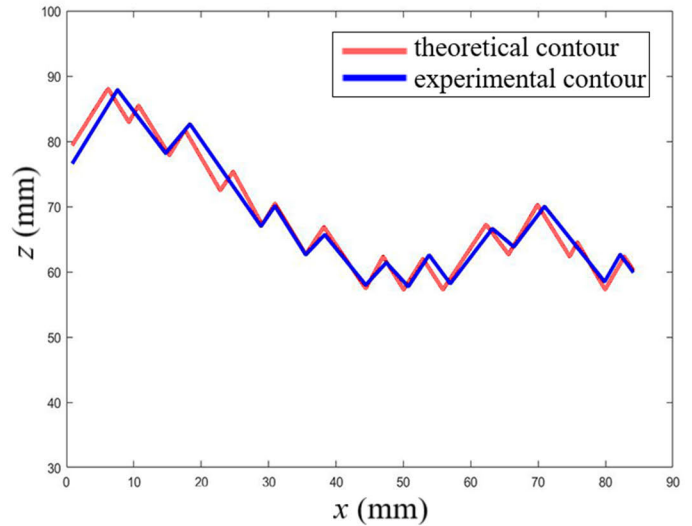
It is also found that the stiffness of workpiece has a great influence on cutting quality. The experimental result shows that the cutting quality of middle position is better than that of edge position; the cutting quality of the first feed of one cutting path is better than that of the back feed cutting; the cutting quality of the workpiece with thick honeycomb wall is better than that with thin wall. The reason is that the middle position of the workpiece has better stiffness than edge position; the honeycomb cell structure is complete and has a better stiffness during the first feed of cutting, whereas the



(a) theoretical contour curve



(b) experimental contour curve



(c) Comparison of two curves

FIGURE 14. Extracting and comparing the contour curves.

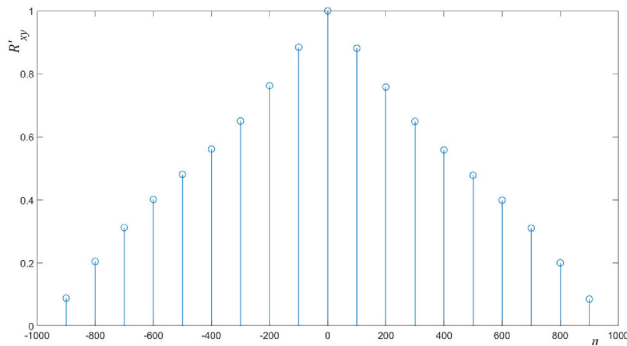


FIGURE 15. Normalized cross-correlation of the two curves.

stiffness decreases during the back feed; the overall stiffness of the workpiece with thicker wall is greater than that with thinner wall.

V. CONCLUSION

In this paper, the V-shaped cutting process is analyzed, and the problem of automatic path planning and generating for V-shaped cutting is solved. To realize the automatic path planning of V-shaped robotic cutting by straight blade tool, the cutting path of cylindrical parts and planning method

for the six DOFs of the straight blade tool are discussed. Then a special post-processing program is developed to transform the milling files into the V-shaped cutting files. The generated robot machining files are lastly verified by kinematic simulation and robotic cutting experiments. Following conclusions are drawn:

1. A path planning method for V-shaped cutting of cylindrical Nomex honeycomb parts is proposed by analyzing the different tool position lattices. The method for determining the path parameters is given. A constrained optimization model of path parameters is established to find the optimal parameters for the highest machining efficiency.
2. A method with general CAM software and specific post-processing is presented to realize path planning of V-shaped cutting. Three-axis reciprocating milling process is pre-generated and then post-processed into V-shaped cutting process based on code recognition and modification of machining files.
3. Simulation and experiment results verify the effectiveness of the proposed method. The motion of robot and the tool path simulated by MATLAB are consistent with the expectation of V-shaped cutting process. Cross-correlation analysis of the experimental result

shows that the machined contour matched the theoretical contour well.

REFERENCES

- [1] C. C. Foo, G. B. Chai, and L. K. Seah, "Mechanical properties of nomex material and nomex honeycomb structure," *Compos. Struct.*, vol. 80, no. 4, pp. 588–594, Oct. 2007, doi: [10.1016/j.compstruct.2006.07.010](https://doi.org/10.1016/j.compstruct.2006.07.010).
- [2] D. D. Gill, D. M. Yip-Hoi, M. Meaker, T. Boni, E. L. Eggeman, A. M. Brennan, and A. Anderson, "Studying the mechanisms of high rates of tool wear in the machining of aramid honeycomb composites," in *Proc. ASME Int. Manuf. Sci. Eng. Conf.*, vol. 50732, Jun. 2017, Art. no. V002T03A002, doi: [10.1115/MSEC2017-2694](https://doi.org/10.1115/MSEC2017-2694).
- [3] M. Jaafar, S. Atlati, H. Makich, M. Nouari, A. Moufki, and B. Julliere, "A 3D FE modeling of machining process of nomex honeycomb core: Influence of the cell structure behaviour and specific tool geometry," *Procedia CIRP*, vol. 58, pp. 505–510, Jan. 2017, doi: [10.1016/j.procir.2017.03.255](https://doi.org/10.1016/j.procir.2017.03.255).
- [4] W. Cui and J. Gao, "Application of ultrasonic cutting technology in the field of composite material processing," (in Chinese), *Aeron. Manuf. Technol.*, vol. 2006, no. 6, pp. 108–109, Jun. 2006, doi: [10.3969/j.issn.1671-833X.2008.04.008](https://doi.org/10.3969/j.issn.1671-833X.2008.04.008).
- [5] X. P. Hu, B. H. Yu, X. Y. Li, and N. C. Chen, "Research on cutting force model of triangular blade for ultrasonic assisted cutting honeycomb composites," in *Proc. 1st CIRP CCMPM*, 2017, pp. 159–163, doi: [10.1016/j.procir.2017.03.283](https://doi.org/10.1016/j.procir.2017.03.283).
- [6] Y. Xia, J. Zhang, Z. Wu, P. Feng, and D. Yu, "Study on the design of cutting disc in ultrasonic-assisted machining of honeycomb composites," *IOP Conf. Ser., Mater. Sci. Eng.*, vol. 611, Oct. 2019, Art. no. 012032, doi: [10.1088/1757-899x/611/1/012032](https://doi.org/10.1088/1757-899x/611/1/012032).
- [7] *Ultrasonic Cutting of Honeycomb*. Accessed: Jul. 29, 2020. [Online]. Available: <https://www.creno-industry.com/ultrasonic/>
- [8] X. Wu, X. Hu, B. Yu, H. Ji, Z. Lu, and X. Xia, "Design of ultrasonic cutting tool for an ultrasonic assisted cutting process of Nomex honeycomb materials based on substitution method," (in Chinese), *China Mech. Eng.*, no. 6, pp. 809–813, 2015, doi: [10.3969/j.issn.1004-132X.2015.06.019](https://doi.org/10.3969/j.issn.1004-132X.2015.06.019).
- [9] H. Ji, W. Yu, X. Hu, and B. Yu, "Influences of cutting tool load on impedance characteristics of honeycomb composite material ultrasonic cutting acoustic system," (in Chinese), *China Mech. Eng.*, vol. 27, no. 18, pp. 2507–2512, 2016, doi: [10.3969/j.issn.1004-132X.2016.18.016](https://doi.org/10.3969/j.issn.1004-132X.2016.18.016).
- [10] X. Huang, X. Hu, B. Yu, and S. Wu, "Research on ultrasonic cutting mechanism of nomex honeycomb composites based on fracture mechanics," (in Chinese), *J. Mech. Eng.*, vol. 51, no. 23, pp. 205–212, 2015, doi: [10.3901/JME.2015.23.205](https://doi.org/10.3901/JME.2015.23.205).
- [11] D. Kang, P. Zou, H. Wu, J. Duan, and W. Wang, "Study on ultrasonic vibration-assisted cutting of nomex honeycomb cores," *Int. J. Adv. Manuf. Technol.*, vol. 104, nos. 1–4, pp. 979–992, Sep. 2019, doi: [10.1007/s00170-019-03883-z](https://doi.org/10.1007/s00170-019-03883-z).
- [12] X. Huang, X. Hu, and B.-H. Yu, "Ultrasonic cutting force model of honeycomb composites and selection of the processing parameters," (in Chinese), *Chin. J. Mech. Electr. Eng.*, vol. 32, no. 1, pp. 32–36, Jan. 2015.
- [13] Y. Zhang, C. Zhang, and W. Li, "Research on NC programming based on CATIA V5 of ultrasonic milling machine tool for composites honeycomb part," (in Chinese), *Aeron. Manuf. Technol.*, vol. 405, no. 9, pp. 79–82, Sep. 2012, doi: [10.16080/j.issn1671-833x.2012.09.025](https://doi.org/10.16080/j.issn1671-833x.2012.09.025).
- [14] R. Kang, Z. Dong, Y. Wang, X. Zhu, K. Han, X. Wang, and Z. Jia, "Honeycomb core lug boss structure ultrasonic cutting method, involves cutting remaining ultrasonic sheet by utilizing circular-sheet knife to obtain honeycomb core lug boss structure with high quality," (in Chinese), CN Patent CN 108 356 289, Aug. 3, 2018.
- [15] L. Chen, Q. Gao, X. Yuan, J. Zhou, S. Ding, L. Sheng, and J. Song, "Method for processing narrow-length beam honeycomb core portion, involves using dagger knife to cut outline of honeycomb core portion axially along outer contour line of portion to realize processing of narrow-length beam core portion," (in Chinese), CN Patent CN 109 304 579-A, Feb. 5, 2019.
- [16] H. Yu, X. Hu, L. Kong, and B. Yu, "Process path planning based on efficiency model for ultrasonic cutting curved surface of honeycomb composite parts," *Adv. Mech. Eng.*, vol. 11, no. 10, pp. 1–11, Oct. 2019, doi: [10.1177/1687814019884176](https://doi.org/10.1177/1687814019884176).
- [17] S. Chen, "The research of the key technology on curved surface forming of honeycomb composite material based on NC ultrasonic cutting," M.S. thesis, Dept. Mech. Eng., Hangzhou Dianzi Univ., Hangzhou, China, 2012.
- [18] E. Liu, X. Hu, and B. Yu, "Research and development of ultrasonic CNC cutting path generation system for nomex composite materials," *Adv. Mater. Res.*, vols. 941–944, pp. 1968–1972, Jun. 2014, doi: [10.4028/www.scientific.net/AMR.941-944.1968](https://doi.org/10.4028/www.scientific.net/AMR.941-944.1968).
- [19] SONIMAT. *Composite & Honeycomb Core Cutting and Machining*. Accessed: Jul. 29, 2020. [Online]. Available: <https://www.sonimat.com/en/composite-cutting-and-welding/products/soniblade-embeddable-end-effector-for-ultrasonic-cutting/>
- [20] T. Gao, J. Luo, Y. Lin, and Y. Li, "Research on CNC machining technology of honeycomb core based on ultrasonic machine tool," (in Chinese), *Machinery*, vol. 51, no. 1, pp. 41–43, Jan. 2013, doi: [10.3969/j.issn.1000-4998.2013.01.015](https://doi.org/10.3969/j.issn.1000-4998.2013.01.015).
- [21] Y. Chen and F. Dong, "Robot machining: Recent development and future research issues," *Int. J. Adv. Manuf. Technol.*, vol. 66, nos. 9–12, pp. 1489–1497, Jun. 2013, doi: [10.1007/s00170-012-4433-4](https://doi.org/10.1007/s00170-012-4433-4).
- [22] Y. Wang, X. Wang, R. Kang, J. Sun, Z. Jia, and Z. Dong, "Analysis of influence on ultrasonic-assisted cutting force of nomex honeycomb core material with straight knife," *J. Mech. Eng.*, vol. 53, no. 19, pp. 73–82, 2017, doi: [10.3901/JME.2017.19.073](https://doi.org/10.3901/JME.2017.19.073).
- [23] A. Olabi, R. Bearee, E. Nyiri, and O. GIBARU, "Enhanced trajectory planning for machining with industrial six-axis robots," in *Proc. IEEE Int. Conf. Ind. Technol.*, Viña del Mar, Chile, Mar. 2010, pp. 500–506, doi: [10.1109/ICIT.2010.5472749](https://doi.org/10.1109/ICIT.2010.5472749).
- [24] W. Xiao, H. Strauß, T. Loohß, H.-W. Hoffmeister, and J. Hesselbach, "Closed-form inverse kinematics of 6R milling robot with singularity avoidance," *Prod. Eng.*, vol. 5, no. 1, pp. 103–110, Feb. 2011, doi: [10.1007/s11740-010-0283-9](https://doi.org/10.1007/s11740-010-0283-9).
- [25] S. Mousavi, V. Gagnol, B. C. Bouzgarrou, and P. Ray, "Dynamic modeling and stability prediction in robotic machining," *Int. J. Adv. Manuf. Technol.*, vol. 88, nos. 9–12, pp. 3053–3065, Feb. 2017, doi: [10.1007/s00170-016-8938-0](https://doi.org/10.1007/s00170-016-8938-0).
- [26] S. Mitsi, K.-D. Bouzakis, G. Mansour, D. Sagris, and G. Maliaris, "Off-line programming of an industrial robot for manufacturing," *Int. J. Adv. Manuf. Technol.*, vol. 26, no. 3, pp. 262–267, Aug. 2005, doi: [10.1007/s00170-003-1728-5](https://doi.org/10.1007/s00170-003-1728-5).
- [27] J. D. Posada, U. Schneider, A. Sridhar, and A. Verl, "Automatic motion generation for robotic milling optimizing stiffness with sample-based planning," *Machines*, vol. 5, no. 1, p. 3, Jan. 2017, doi: [10.3390/machines5010003](https://doi.org/10.3390/machines5010003).
- [28] P. Corke, "Robot arm kinematics," in *Springer Tracts in Advanced Robotics*, vol. 118. Cham, Switzerland: Springer, 2017, pp. 137–170.
- [29] K. Ma, J. Zhang, P. Feng, Z. Wu, D. Yu, and S. Ahmad, "Design and implementation of a mini ultrasonic cutting system for nomex honeycomb composites," in *Proc. 16th Int. Bhurban Conf. Appl. Sci. Technol.*, M. ZafarUzZaman, Ed., Islamabad, Pakistan, 2019, pp. 148–152, doi: [10.1109/IBCAST.2019.8667261](https://doi.org/10.1109/IBCAST.2019.8667261).



RUOYU CUI was born in Gansu, China, in 1997. He received the B.S. degree in mechanical engineering from Tsinghua University, China, in 2019, where he is currently pursuing the Ph.D. degree with the Department of Mechanical Engineering. He is mainly involved in the research of ultrasonic machining of composite parts. His research interests include mechanical processes and industrial robots.



JIANFU ZHANG (Member, IEEE) received the Ph.D. degree in mechanical engineering from Tsinghua University, China, in 2009. He is currently an Associate Professor and also a Doctoral Supervisor with the Department of Mechanical Engineering, Tsinghua University. He has undertaken more than 20 national, provincial, and industrial projects. His main research interests include precision processing technology and equipment, ultrasonic machining technology, and intelligent manufacturing technology. He has won seven provincial and ministerial awards, published more than 150 articles, applied for/obtained more than 40 patents for invention, and achieved 20 software copyrights.



DINGWEN YU is currently a Professor and also a Doctoral Supervisor with the Department of Mechanical Engineering, Tsinghua University, China. He has published more than 160 articles, applied for/obtained more than 40 patents for invention, and achieved 20 software copyrights. He has participated in and undertook more than 20 national “973” basic research projects, 863 national projects, major national science and technology projects, and national defense pre-research projects. His main research interests include analysis and design of dynamic characteristics of mechanical systems, manufacturing information, and system integration technology.



PINGFA FENG received the Ph.D. degree in mechanical engineering from the Department of Transportation and Mechanical Systems, Technical University of Berlin, Germany, in 2003. He is currently a Professor and also a Doctoral Supervisor with the Department of Mechanical Engineering, Tsinghua University, China. He has completed or is in charge of more than 20 national 973 programs, 863 programs, major projects, natural science funds, and international cooperation projects, published one monograph and 200 articles, applied for/obtained more than 40 patents for invention, and achieved 20 software copyrights. His main research interests include precision processing technology, intelligent manufacturing, and manufacturing equipment performance analysis and optimization.



ZHIJUN WU is currently a Professor with the Department of Mechanical Engineering, Tsinghua University, China. He has participated in and undertook 18 projects such as the National Natural Science Foundation, the National Science and Technology Major Special Project, the Beijing Natural Science Foundation, and the Beijing Science and Technology Program. He has published more than 150 articles, applied for/obtained more than 40 patents for invention, and achieved 20 software copyrights. His main research fields are precision processing technology and equipment, and manufacturing information and system integration technology.

...